# MicroRNA-153 may act as a potential biomarker and prognostic indicator of patients with gastric cancer

TIAN LI[1], DONG GUO[2], XIAOYAN XU[1], PENG LIU[2], PING WANG[1], YONGCUN ZHU[3], LIN LIN[1], YEMIN QU[2], FENG LIU[1], YANLIU CHU[1] and XIAOZHONG GAO[1]

Departments of [1]Gastroenterology, [2]Central Lab and [3]Pathology, Weihai Municipal Hospital, Cheeloo College of Medicine, Shandong University, Weihai, Shandong 264200, P.R. China

Received August 14, 2022; Accepted April 5, 2023

DOI: 10.3892/ol.2023.13864

**Abstract.** MicroRNA (miR/miRNA)-153, as a novel tumor-related miRNA, has been found to be aberrantly expressed in different types of cancer; however, to the best of our knowledge, the role of miR-153 in gastric cancer (GC) remains unclear. The present study demonstrated that miR-153 expression was markedly decreased in GC, including GC cell lines and culture medium, GC tissues, and serum samples, based on reverse transcription-quantitative PCR, and this was further confirmed by fluorescence *in situ* hybridization. Transfection with miR-153 mimics inhibited proliferation and migration, and promoted apoptosis in GC cells. The serum expression levels of miR-153 were decreased in 59 patients with GC compared with those of 9 healthy controls, and more decreased in advanced GC compared with early-stage GC, suggesting that miR-153 was associated with tumor progression. Furthermore, serum miR-153 was expressed at significantly lower levels in patients with GC with larger tumor size (≥4 cm; P=0.013), poor differentiation and signet histology (P=0.013), lymph node metastasis (P=0.025) and advanced tumor stage (TNM stage III and IV; P=0.048) compared with patients with a smaller tumor size (<4 cm), well and moderate differentiation, no lymph node metastasis, and TNM stage I and II, respectively. In conclusion, the present study revealed that low miR-153 expression was associated with poor prognosis in GC and miR-153 may potentially act as a tumor biomarker and therapeutic target in GC.

*Correspondence to:* Professor Xiaozhong Gao or Professor Yanliu Chu, Department of Gastroenterology, Weihai Municipal Hospital, Cheloo College of Medicine, Shandong University, 70 Heping Road, Weihai, Shandong 264200, P.R. China
E-mail: xzgaoweihai@sina.com
E-mail: yanliuchu@163.com

*Key words:* microRNA-153, gastric cancer, proliferation, migration, apoptosis, biomarker, prognosis

## Introduction

Gastric cancer (GC) remains the fifth most common cancer and the third leading cause of cancer-related deaths worldwide (1). Surgical resection of the primary tumor in the stomach is by far the most effective treatment, yet less than half of patients with GC are diagnosed and undergo radical resection at an early stage, which is associated with a 5-year survival rate of up to 90% (2,3). In addition, patients with advanced GC who undergo radical resection have a higher recurrence rate and lower 5-year survival rate (~20%) compared with early-stage GC (2,3). The use of sensitive methods and specific tumor biomarkers for early detection of GC and monitoring the risk of recurrence can markedly improve the prognosis of patients with GC. However, the existent biomarkers for GC are mostly non-specific, as they are also elevated in other malignant tumors and certain benign diseases (4). Therefore, it is necessary to find novel biomarkers to improve the early diagnosis rate of GC.

MicroRNAs (miRs/miRNAs), which are 18-22 nucleotides in length, are considered a large class of evolutionarily conserved non-coding RNAs, which can regulate target genes and serve critical roles in a number of essential cell processes, including proliferation, differentiation, development, survival and death (5). Previous studies have demonstrated that miRNAs serve a key role in the occurrence and development of cancer (6-11). Numerous cancer types, including liver cell carcinoma, papillary thyroid carcinoma, lung cancer, glioblastoma, breast cancer, colorectal cancer and lymphoma, have been demonstrated to exhibit dysregulation of miRNAs to promote or inhibit tumor progression, which suggests that miRNAs could be potential biomarkers of cancer (7-11).

Dysregulation of miR-153 has previously been observed in several common human cancer types, with evidence indicating that miR-153 can serve as an oncogene in colorectal cancer, hepatocellular carcinoma and prostate cancer (12-14) or as a tumor suppressor gene in glioma, nasopharyngeal cancer, breast cancer and laryngeal carcinoma (15-19). Therefore, the functional role of miR-153 in cancer development and progression is cancer type-specific. In addition, the clinical role of miR-153 in GC and its expression in the serum of patients with GC have not been elucidated clearly. The present study aimed to investigate miR-153 expression in tissues and serum samples

of patients with GC, and to identify the association between miR-153 expression and clinicopathological characteristics of patients with GC.

## Materials and methods

*Cells and cell culture*. The GES-1 human gastric epithelial cell line and the HGC-27, AGS and MKN-28 human GC cell lines were obtained from BeNa Culture Collection; Beijing Beina Chunglian Institute of Biotechnology (Beijing, China). MKN-28 cells were authenticated by BeNa Culture Collection; Beijing Beina Chunglian Institute of Biotechnology by short tandem repeat profiling. All cells were cultured in RPMI-1640 medium (HyClone; Cytiva) with 10% FBS (Biological Industries; Sartorius AG) at 37˚C in a humidified incubator with 5% $CO_2$.

*Patient tissue and blood sample preparation*. In the present study, clinical tissues of 20 patients (age range, 40-77 years) and blood samples of 59 patients with GC (age range, 40-77 years) and 9 healthy controls (HCs; age range, 38-72 years) were collected from Weihai Municipal Hospital, Shandong University (Weihai, China) between January 2021 and January 2022. Clinicopathological data are presented in Table I. Strict inclusion and exclusion criteria were established for patients with GC. The inclusion criteria were: i) 18-80 years old; and ii) patients were diagnosed by endoscopic biopsy or surgery according to the World Health Organization pathological classification (20). The exclusion criteria were as follows: i) History of other malignant tumors; ii) history of any kind of preoperative treatment, including radiotherapy, chemotherapy and immunotherapy; and iii) severe liver and kidney diseases such as liver failure and kidney failure, endocrine and metabolic diseases such as diabetes and hypertension, and other connective tissue diseases such as systemic lupus erythematosus. After screening, a total of 59 patients with GC were enrolled and GC tissues and matched adjacent non-cancerous tissues were obtained from surgical resected gastric tissues from 20 of these patients and immediately snap-frozen in dry ice and stored at -80˚C.

Blood samples were obtained from 59 patients with GC (25 patients with early-stage GC, including high-grade intraepithelial neoplasia and low-grade intraepithelial neoplasia, and 34 patients with advanced GC stages) and 9 HCs. HCs were identified by clinical manifestations, disease history and blood test results. The inclusion criteria for HCs were: i) 18-80 years old; ii) no sex restriction; and iii) volunteers who were in good physical condition. The exclusion criterion was history of disease and surgery. Blood samples were centrifuged at 900 x g (iCEN-24R; Hangzhou Allsheng Instruments Co., Ltd.) at 20˚C for 10 min for serum separation and stored at -80˚C prior to small RNA isolation. The study was approved by the Ethics Committee of Weihai Municipal Hospital (approval number 2020010; Weihai, China) and written informed consent was obtained from all patients and HCs.

*Reverse transcription-quantitative PCR (RT-qPCR)*. Small RNAs were extracted from cells and tissues using RNAiso for Small RNA (Takara Bio, Inc.) according to the manufacturer's protocol. The synthetic cel-miR-39-3p standard RNA (Guangzhou RiboBio Co., Ltd.) was adopted as the external reference. Small RNAs were isolated from the serum with the Serum/Plasma miRNA Extraction Kit (HaiGene Biotech Co., Ltd.) according to the manufacturer's instructions. The optical density (OD) of the extracted RNA was measured with a NanoDrop spectrophotometer (Thermo Fisher Scientific, Inc.) at 260 and 280 nm. Both the tissue and serum small RNAs ($OD_{260/280}$ >1.8) were then converted into the reverse transcription product using a HiFiScript cDNA Synthesis Kit (cat. no. CW2569M; CoWin Biosciences) using specific primers (confidential sequences; cat. no. F02002; Suzhou GenePharma Co., Ltd.) according to the manufacturer's instructions. miRNA expression was then examined using the UltraSYBR Mixture kit Low ROX (CoWin Biosciences) on the thermocycler ABI 7500 (Thermo Fisher Scientific, Inc.). For the determination of serum miRNA expression, miR-39 was used as the external reference, while U6 was used as the internal reference for the determination of tissue miRNA expression. The sequences of miR-153 and U6 primers (Suzhou GenePharma Co., Ltd.) were as follows: hsa-miR-153-3p forward, 5'-AACGAACTTGCATAGTCACAAAAG-3' and reverse, 5'-TATGGTTTTGACGACTGTGTGAT-3'; and U6 forward, 5'-CAGCACATATACTAAAATTGGAACG-3' and reverse, 5'-ACGAATTTGCGTGTCATCC-3'. The sequence of the primers for miR-39 is confidential and the design method has been patented (cat. no. MQPS0000071-1-100; Guangzhou RiboBio Co., Ltd.). qPCR was performed at 95˚C for 10 min, followed by 40 cycles of denaturation for 15 sec and annealing/elongation at 60˚C for 1 min. All reactions were repeated at least three times and the $2^{-\Delta\Delta Cq}$ method was used to analyze the relative expression (21).

*miRNA sequencing*. To examine the potential significance of miRNAs in GC, we sent several pairs of tissues for sequencing. We required OD 260/280 >1.8 and a complete sample band visible on the agarose gel electrophoresis image to verify the quality of samples. Finally, the miRNA profiles in three GC tissues and matched adjacent non-tumor tissues were determined by miRNA sequencing with the Hiseq Rapid SBS Kit V2 (50 cycle) (cat. no. FC-402-4022; Illumina, Inc.) and Hiseq Rapid SR Cluster Kit V2 (cat. no. GD-402-4002; Illumina, Inc.). Total RNA was isolated from cells using a Magzol Reagent kit (cat. no. R4801; Magen Biotechnology Co., Ltd.) according to the manufacturer's protocol. The quantity and integrity of the RNA yield was assessed by using the K5500 (Beijing Kaiao Technology Development Co., Ltd.) and the Agilent 2200 TapeStation (Agilent Technologies, Inc.). Briefly, total RNA was ligated with 3' and 5' adapters. Subsequently, the adapter-ligated RNAs were subjected to RT-PCR and amplified with 12 cycles. The sequences of the primers were forward, 5'-AATGATACGGCGACCACCGAGATCTAC ACGTTCAGAGTTCTACAGTCCGA-3' and reverse, 5'-CAA GCAGAAGACGGCATACGAGATCGTGATGTGACTGGA GTTCCTTGGCACCCGAGAATTCCA-3'. PCR products were size-selected using an 8% agarose gel according to instructions of the NEBNext® Multiplex Small RNA Library Prep Set for Illumina® (cat. no. E7560; Illumina, Inc.). The purified library products were evaluated using the Agilent 2200 TapeStation and a Qubit fluorometer (Thermo Fisher

Table I. Demographic data of all patients.

| Clinicopathological features | Tissue samples of patients with GC (n=20) | Serum samples | |
|---|---|---|---|
| | | Patients with GC (n=59) | Healthy controls (n=9) |
| Sex | | | |
| Male | 14 | 34 | 5 |
| Female | 6 | 25 | 4 |
| Age, years | 63.851±9.438 | 64.118±7.704 | 56.453±11.396 |
| Histology | | | |
| Well, moderate | 13 | 33 | - |
| Poor, signet | 7 | 26 | - |
| Tumor size, cm | | | |
| <4 | 8 | 34 | - |
| ≥4 | 12 | 25 | - |
| Lymph node metastasis | | | |
| Absent | 7 | 40 | - |
| Present | 13 | 19 | - |
| TNM stage | | | |
| I, II | 11 | 43 | - |
| III, IV | 9 | 16 | - |

Values are expressed as n or the mean ± standard deviation. GC, gastric cancer.

Scientific, Inc.). The loading concentrations of the final library (Table II) were measured using a Qubit dsDNA HS Assay Kit (cat. no. Q32854; Invitrogen; Thermo Fisher Scientific, Inc.) to quantify the concentration in ng/$\mu$l first, and then converted to molar concentrations using the formula. The sequencing was outsourced to Guangzhou RiboBio Co., Ltd. and was performed with an Illumina instrument (Illumina, Inc.; single-end; 50 bp).

*Bioinformatics analysis*. The raw reads were processed by filtering out reads containing adapters, poly 'N', low quality reads and reads of <17 nucleotides using FastQC (version 0.11.2; https://www.bioinformatics.babraham.ac.uk/projects/fastqc/) to obtain clean reads. Mapping of clean reads to the reference genome (hg19; https://www.ncbi.nlm.nih.gov/data-hub/genome/GCF_000001405.25/) was completed using Bowtie (version 1.1.1; https://sourceforge.net/projects/bowtie-bio/). MiRDeep2 (version miRDeep2.0.0.8; https://github.com/rajewsky-lab/mirdeep2/) was used to identify known mature miRNAs based on miRBase22 (www.miRBase.org) and to predict novel miRNAs. Databases, including Rfam12.1 (http://ftp.ebi.ac.uk/pub/databases/Rfam/12.1/) and pirnabank (http://pirnabank.ibab.ac.in/), were used to identify ribosomal RNA, transfer RNA, small nuclear RNA, small nucleolar RNA and piwi-interacting RNA using BLAST (version 2.2.30+; https://ftp.ncbi.nlm.nih.gov/blast/executables/blast+/2.2.30/). The miRNA expression was calculated as reads per million values. Differential expression between two sets of samples was calculated using the edgeR algorithm (version 33.20.9; http://www.bioconductor.org/packages/release/bioc/html/edgeR.html) according to the criteria of log2(fold change)≥1 and P<0.05. The heat map of the top 10 upregulated and downregulated miRNAs with the highest absolute fold-change values was analyzed using pheatmap (version 1.0.12; https://www.rdocumentation.org/packages/pheatmap/versions/1.0.12/topics/pheatmap) and R (version 3.5.0; http://www.r-project.org/).

*Fluorescence in situ hybridization (FISH)*. FISH for miR-153 was performed on paraffin sections using a Fluorescent *In Situ* Hybridization Kit (cat. no. F43501; Suzhou GenePharma Co., Ltd.) and the CY3®-labeled locked nucleic acid (LNA) probe (Suzhou GenePharma Co., Ltd.) according to the manufacturer's protocol. The probe sequence (5'-3') was GATCACT+TTTGTGAC+TATGCAA, where + means LNA modification. First, the dissected tissues were fixed with 10% formalin for 48 h at room temperature. After rinsing the tissues with running tap water and dehydrating these in 70, 95 and 100% ethanol successively, these were incubated in a 65˚C paraffin bath twice for 30 min each. Subsequently, the paraffin-embedded tissues were sectioned into 4-$\mu$m-thick slices. Briefly, the paraffin sections were dewaxed and rehydrated using a graded series of ethanol (100, 95, 90, 80 and 70%) for 10 min each at room temperature, and digested with proteinase K (GenePharma) for 20 min at 37˚C. After washing three times with 100 $\mu$l 2X Buffer C for 1 min each at room temperature, each sample was denatured with 100 $\mu$l 0.1% 2X Buffer C and 0.7% Buffer D for 8 min at 78˚C. Each sample was incubated successively with 70, 80, 90 and 100% ethanol for 2 min at room temperature. After drying at room temperature, hybridization was performed overnight at 37˚C with 100 $\mu$l denatured

Table II. Final library concentrations.

| No. | Samples | Testing result | | | Test conclusion |
|---|---|---|---|---|---|
| | | Main peak size, bp | Mass concentration, ng/$\mu$l | Molar concentration, x$10^3$ pmol/l | |
| 1 | GC-1 | 168 | 7.66 | 70.3 | Pass |
| 2 | Adjacent-1 | 163 | 2.71 | 25.6 | Pass |
| 3 | GC-2 | 167 | 13.4 | 123 | Pass |
| 4 | Adjacent-2 | 163 | 2.74 | 25.9 | Pass |
| 5 | GC-3 | 165 | 3.12 | 29 | Pass |
| 6 | Adjacent-3 | 160 | 4.62 | 44.5 | Pass |

GC, gastric cancer.

Table III. Association between clinicopathological features and miR-153 expression in the serum of 59 patients with GC.

| Clinicopathological features | All patients with GC, n (n=59) | miR-153 expression, mean ± SD | t | P-value |
|---|---|---|---|---|
| Age, years | | | 0.441 | 0.661 |
| <65 | 32 | 0.717±0.964 | | |
| ≥65 | 27 | 0.610±0.886 | | |
| Sex | | | -1.700 | 0.095 |
| Male | 34 | 0.496±0.784 | | |
| Female | 25 | 0.903±1.055 | | |
| Histology | | | 2.614 | 0.013[a] |
| Well, moderate | 33 | 0.909±1.162 | | |
| Poor, signet | 26 | 0.363±0.272 | | |
| Tumor size, cm | | | 2.602 | 0.013[a] |
| <4 | 34 | 0.895±1.141 | | |
| ≥4 | 25 | 0.361±0.308 | | |
| Lymph node metastasis | | | -2.303 | 0.025[a] |
| Absent | 40 | 0.805±1.080 | | |
| Present | 19 | 0.381±0.298 | | |
| TNM stage | | | 2.022 | 0.048[a] |
| I, II | 43 | 0.766±1.051 | | |
| III, IV | 16 | 0.406±0.311 | | |

[a]Statistically significant. P-values were obtained using an unpaired t-test (mean expression values were compared). GC, gastric cancer; miR, microRNA.

5' CY3-labeled LNA probe (2 $\mu$M) targeted at miR-153 in 1X Buffer E (The probe with Buffer E was preincubated for denaturation at 73˚C for 5 min). To remove excess probes, one wash was performed with 100 $\mu$l 0.1% 2X Buffer C and 0.5% Buffer D for 15 min at 43˚C, followed by two washes with 100 $\mu$l 2X Buffer C for 10 min at 37˚C, and one wash with PBS for 10 min at room temperature. The sections were counterstained with DAPI at room temperature for 20 min after washing, and were observed under a fluorescence microscope (Nikon ECLIPSE Ti; Nikon Corporation) and analyzed using ImageJ software (version 1.8.0.112; National Institutes of Health).

*Cell transfection*. Cells (2x$10^5$ cells per well) were inoculated in a 6-well plate at 37˚C in a humidified atmosphere containing 5% $CO_2$ and transfected with synthetic miR-153 mimics (sense, 5'-UUGCAUAGUCACAAAAGUGAUC-3'; antisense, 5'-UCACUUUUGUGACUAUGCAAUU-3'), inhibitors (5'-GAUCACUUUUGUGACUAUGCAA-3'), scrambled mimics negative controls (NCs; sense, 5'-UUCUCCGAACGUGUCACGUTT-3'; antisense, 5'-ACGUGACACGUUCGGAGAATT-3') or scrambled inhibitor NCs (InNCs; 5'-CAGUACUUUUGUGUAGUACAA-3'), which were all purchased from Shanghai GenePharma Co., Ltd., at a concentration of 100 nM using Lipofectamine® 2000 (Invitrogen; Thermo Fisher Scientific,

Inc.). Following incubation at 37˚C for 5-8 h, the transfection solution was removed. Functional experiments were conducted 24-48 h post-transfection. The transfection efficiency was assessed by RT-qPCR.

*Wound-healing assay*. Migration was evaluated using a wound healing assay. Briefly, AGS and GES-1 cells ($2x10^5$ cells per well) were inoculated into a 24-well plate and cultured to 90% confluence. Subsequently, a line-shaped wound was created using a sterile pipette tip, and cells were washed using PBS. The cells were then incubated in RPMI-1640 without FBS at 37˚C for 48 h. Images of cell migration were captured at 0, 24 and 48 h under an inverted light microscope (magnification, x10) and analyzed using the ImageJ (version 1.8.0.112; National Institutes of Health). The percentage of wound gap closure was calculated as follows: Wound healing rate (migration area)=$(A_0-An)/A_0$, where $A_0$ represents the initial wound area, and An represents the remaining area of the wound at the timepoint examined.

*Apoptosis assay*. Cells were collected, resuspended and stained using an Annexin V-FITC apoptosis detection kit [including propidium iodide (PI); cat. no. C1062L; Beyotime Institute of Biotechnology] according to the manufacturer's instructions. Next, cells were detected using a BD FACSAria™ II cell sorter (BD Biosciences) and analyzed using BD FACSDiva software (version 8.0; BD Biosciences).

*5-ethynyl-2-deoxyuridine (EdU) proliferation assay*. This assay was performed using the BeyoClickTM EdU Cell Proliferation Kit with Alexa Fluor 488 (Beyotime Institute of Biotechnology) according to the manufacturer's protocol. AGS cells ($1x10^6$ cells per well) were inoculated in a 6-well plate and labeled with 10 $\mu$M EdU reagent at 37˚C for 2 h. Subsequently, the AGS cells were fixed in 4% paraformaldehyde for 15 min at room temperature and permeabilized with 0.3% Triton X-100 for 15 min. The cells were washed three times using PBS, and cultured with 0.5 ml Click Reaction Mixture for 30 min at room temperature without light. Subsequently, cells were stained with 1 ml DAPI (5 $\mu$g/ml) for 10 min at room temperature, and were imaged using a fluorescence microscope (Nikon ECLIPSE Ti; Nikon Corporation) and analyzed using ImageJ software (version 1.8.0.112; National Institutes of Health).

*Statistical analysis*. Statistical analysis was performed using SPSS (version 24.0; IBM Corp.) and GraphPad Prism (version 7.0; Dotmatics). All experiments were performed independently at least three times and all values are presented as the mean ± SD. An unpaired or paired Student's t-test was used for comparisons between two groups. Comparisons among multiple groups were analyzed using one-way ANOVA followed by Dunnett's or Tukey's post-hoc tests. $P<0.05$ was considered to indicate a statistically significant difference.

## Results

*miR-153 expression in GC and matched adjacent non-tumor tissues*. To screen differentially regulated miRNAs, human miRNA sequencing was conducted in three pairs of GC tissues and matched adjacent tissues. In total, 194 miRNAs were aberrantly expressed with fold change ≥2.0 and $P<0.05$ after normalization. Among them, 124 miRNAs were upregulated and 70 miRNAs were downregulated. The scatter (Fig. 1A) and volcano (Fig. 1B) plots showed the variation in miRNA expression between GC and matched adjacent tissues. In addition, a heat map shows the top 10 miRNAs with the highest absolute fold-change values (Fig. 1C). The literature was reviewed and it was revealed that dysregulation of miR-153 has previously been observed in several common human cancer types, including colorectal cancer, hepatocellular carcinoma and breast cancer (12-19); however, the role of miR-153 in GC remains unclear. The results demonstrated that miR-153-3p was one of the most downregulated miRNAs in GC tissues. miR-153 expression was examined in 20 pairs of GC and matched adjacent non-tumor stomach tissues by RT-qPCR and normalized to an endogenous control (U6). miR-153 expression was downregulated in 17 out of 20 GC tissues compared with matched adjacent non-tumor tissues (Fig. 1D), and the result was further confirmed by FISH (Fig. 1E). Therefore, it was concluded that miR-153 expression in GC was markedly lower than that in paired adjacent tissues, suggesting that miR-153 may function as a tumor suppressor in GC.

*miR-153 expression in cell lines and culture media*. RT-qPCR was performed to evaluate the expression levels of miR-153 in the three GC cell lines (HGC-27, AGS and MKN28) and GES-1 cells, and the culture media. miR-153 expression was lower in GC cell lines (Fig. 2A) and GC cell culture media (Fig. 2B) compared with GES-1 cells and GES-1 culture media, respectively. Therefore, we hypothesized that miR-153 may be secreted outside the cells to serve its role.

*miR-153 inhibits GC cell proliferation and migration, and increases apoptosis in vitro*. The AGS GC cell line was transfected with miR-153 mimics to investigate the role of miR-153 in GC. miR-153 expression was increased in AGS cells transfected with miR-153 mimics (Fig. S1A) and decreased in GES-1 cells transfected with miR-153 inhibitors (Fig. S1B). EdU assays were conducted and revealed that miR-153 upregulation significantly reduced EdU-positive AGS cells (Fig. 2C). Furthermore, wound healing assays were conducted to determine the effect of miR-153 mimics transfection in AGS cells and miR-153 inhibitors transfection in GES-1 cells on migration. A marked reduction in migration of AGS cells was observed when miR-153 was upregulated compared with the mimics NC group. On the other hand, the downregulation of miR-153 resulted in significant promotion of migration of GES-1 cells compared with the inhibitors NC group (Fig. 2D). The effect of miR-153 on GC cell apoptosis was examined using an apoptosis assay. Upregulation of miR-153 resulted in a significant increase in the apoptosis of AGS cells (Fig. 2E). These results demonstrated that miR-153 could inhibit GC cell proliferation and migration, and increase apoptosis *in vitro*.

*Clinical significance of serum expression levels of miR-153 in patients with GC and HCs*. The serum expression levels of miR-153 in 59 patients with GC (25/59 in early GC stage) and 9 HCs were examined by RT-qPCR. The serum expression levels of miR-153 were downregulated in patients with

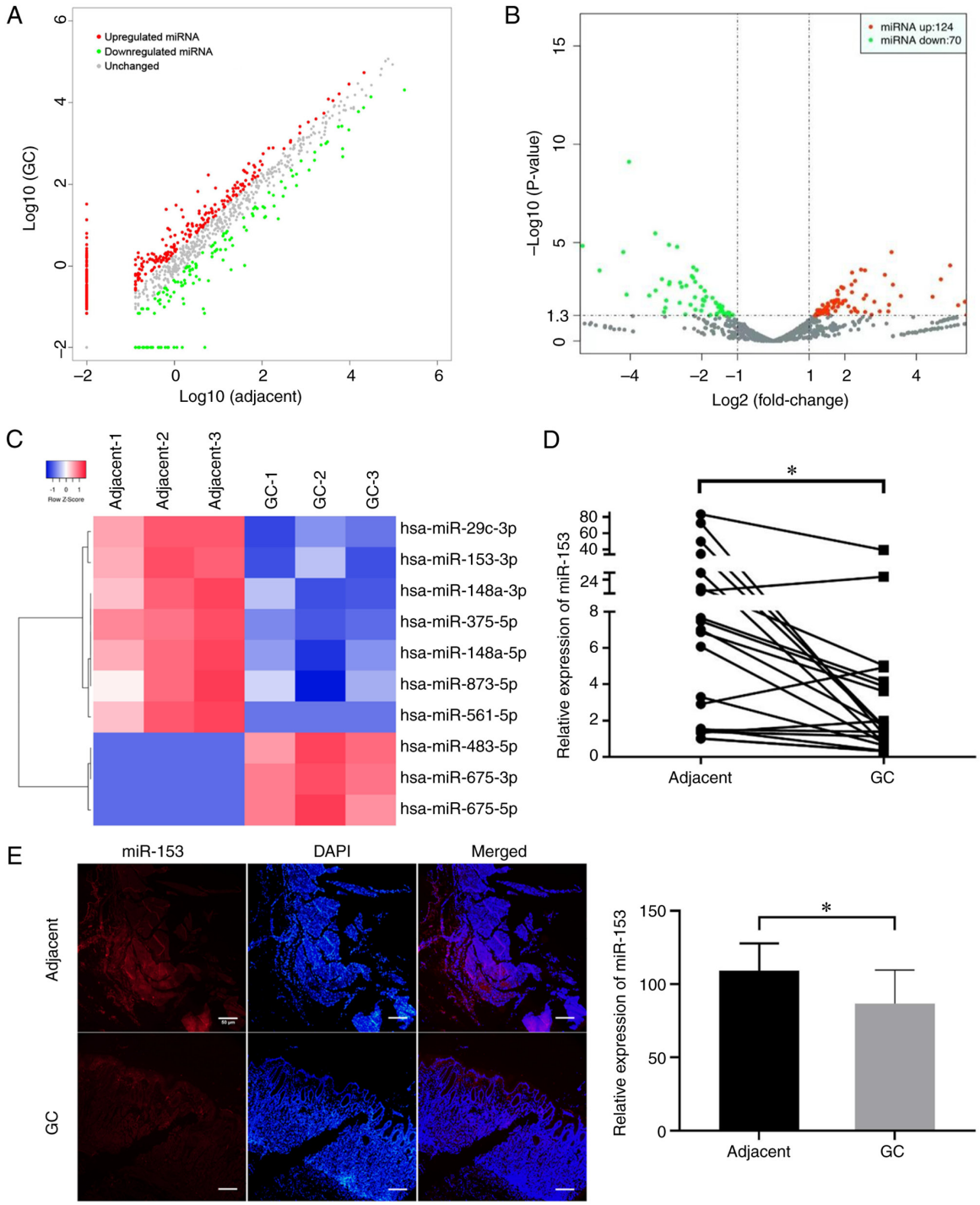


Figure 1. miRNA expression profile in GC. (A) Scatter plots used to assess the variation in the expression of miRNA between GC tissues (GC-1, GC-2 and GC-3) and matched adjacent tissues (Adjacent-1, Adjacent-2 and Adjacent-3). (B) Volcano plot created using fold-change values and P-values. The vertical lines correspond to 2.0-fold upregulation and downregulation, respectively, and the horizontal line represents a P-value of 0.05. (C) Heat map of the top 10 upregulated and downregulated miRNAs with the highest absolute fold-change values in GC tissues compared with in matched adjacent tissues. Red indicates upregulation and blue indicates downregulation. (D) miR-153 expression detected by reverse transcription-quantitative PCR in 20 GC tissues compared with that in matched adjacent non-tumor tissues. (E) Representative images of miR-153 detection by fluorescence *in situ* hybridization. Fluorescence quantification confirmed the decreased expression levels of miR-153 in GC tissues (scale bar, 50 $\mu$m). P-values were obtained using a paired t-test. $^{*}$P<0.05. GC, gastric cancer; miRNA/miR, microRNA.

GC compared with HCs (Fig. 3A). Lower miR-153 expression was identified in patients with advanced GC compared with patients with early GC (Fig. 3B). Serum miR-153 was expressed at significantly lower levels in patients with GC with larger tumor size (≥4 cm), poor differentiation and signet histology, lymph node metastasis and advanced tumor stage [TNM stage (22) III and IV] compared with patients with smaller tumor size (<4 cm), well and moderate differentiation, no lymph node metastasis and TNM stage I and II, respectively, revealing that the downregulation of miR-153 may contribute to GC aggressiveness and poor prognosis (Table III).

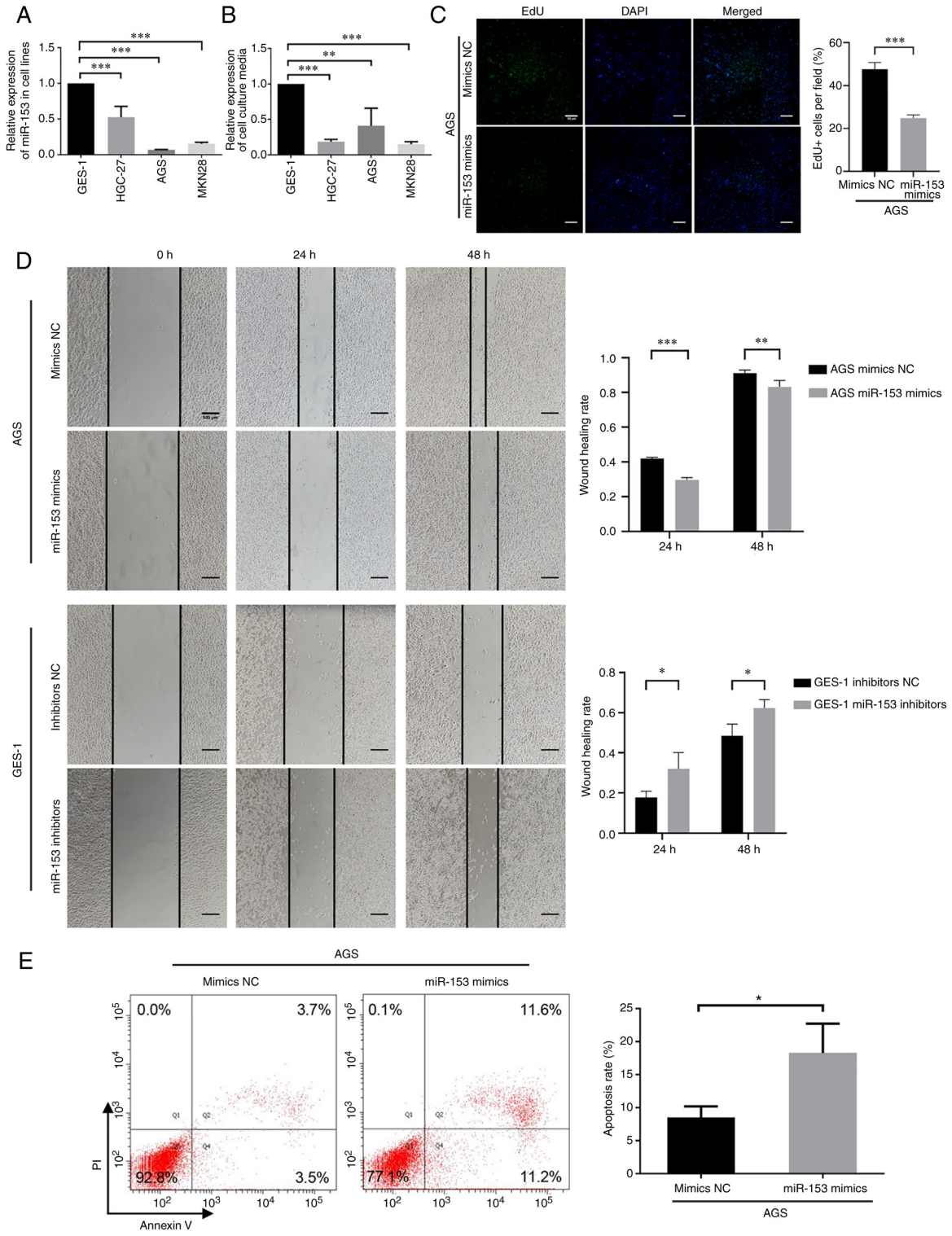


Figure 2. Expression and function of miR-153 in GC cells. miR-153 expression was downregulated in both (A) GC cell lines and (B) their culture media. P-values in (A and B) were obtained using one-way ANOVA followed by Dunnett's post-hoc test. In terms of the function of miR-153 in GC cells, miR-153 could inhibit GC cell proliferation and migration, and increase apoptosis *in vitro*. (C) Representative images of EdU cell proliferation assay (magnification, x20; scale bar, 50 $\mu$m) and the quantification bar plot of the percentage of EdU-positive cells transfected with mimics NC or miR-153 mimics. (D) Wound healing (scale bar, 500 $\mu$m) and (E) apoptosis assays were performed to evaluate the migration and apoptosis of AGS cells, respectively. P-values in (C-E) were obtained using an unpaired t-test. $^{*}$P<0.05; $^{**}$P<0.01; $^{***}$P<0.001. NC, negative control; GC, gastric cancer; miRNA/miR, microRNA; EdU, 5-ethynyl-2-deoxyuridine.

## Discussion

In addition to the multiple genetic and epigenetic changes of protein-coding genes in GC, accumulating evidence indicates that dysregulation of miRNAs serves an important role in the development of GC, including cell proliferation, apoptosis, migration and invasion (2,3). As a member of the miRNA family, several studies have demonstrated that miR-153 contributes to suppression or promotion of cancer cell proliferation, invasion and migration in different cancer

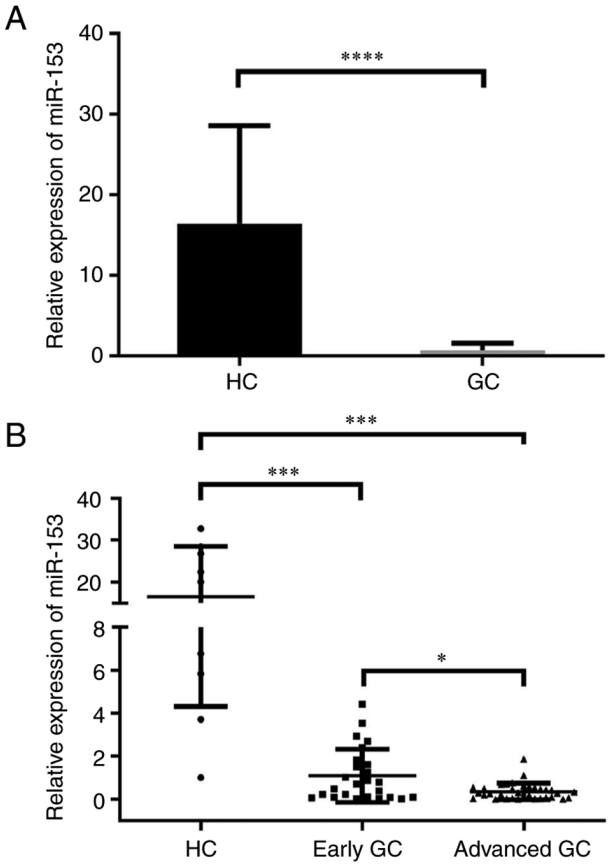


Figure 3. Serum expression levels of miR-153 in patients with GC. (A) Serum expression levels of miR-153 were downregulated in patients with GC compared with HCs. The P-value was obtained using an unpaired t-test. (B) Serum expression levels of miR-153 were lower in patients with advanced GC compared with patients with early GC. P-values were obtained using one-way ANOVA followed by Tukey's test. $^{*}$P<0.05; $^{***}$P<0.001; $^{****}$P<0.0001. GC, gastric cancer; HCs, healthy controls; miR, microRNA.

types, including breast cancer, ovarian cancer and malignant melanoma (17,23,24); however, the molecular mechanism remains unclear.

In the present study, miR-153 expression was significantly downregulated in GC tissues and cell lines compared with matched adjacent non-tumor tissues and GES-1 cells. It was observed that miR-153 could inhibit GC cell proliferation and migration, and increase apoptosis *in vitro*, thus miR-153 downregulation may be a key process in the progression of human GC. Furthermore, miR-153 expression in cell culture media was investigated and a similar trend was observed compared with that of the cell lines, indicating that miR-153 might act as a potent serum clinical diagnostic marker in GC. Based on this finding, the serum expression of miR-153 was detected, and it was shown that it was downregulated in patients with GC and in advanced GC compared with early GC. Accordingly, lower expression of miR-153 was significantly associated with advanced clinical stages of GC and thus poor prognosis. In addition to this, serum miR-153 was expressed at markedly lower levels in patients with GC with poor differentiation, larger tumor sizes, lymph node metastasis and advanced tumor stage. Although the difference of serum miR-153 between TNM stage III/IV and I/II was small (P=0.048), a larger sample size could confirm this finding. These data indicated that miR-153 may be a potential biomarker for the prediction of the prognosis of patients with GC.

Studies have found that epithelial-mesenchymal transition (EMT) serves an important role in the migration and invasion of GC, which leads to a poor prognosis (25-28). Cellular EMT is characterized by loss of cell polarity and intracellular junctions, as well as acquisition of mesenchymal properties. As a result, GC cells migrate and invade more frequently than normal cells (26). By targeting snail family transcriptional repressor 1 (SNAI1) and zinc finger E-box binding homeobox 2, miR-153 is a novel regulator of EMT, suggesting its potential therapeutic value in reducing cancer metastasis (27). Additionally, overexpression of miR-153 significantly reduces GC cell proliferation, migration and invasion (27). According to Zhang *et al* (28), miR-153 overexpression reduced SNAI1 expression and inhibited EMT of GC cells as evidenced by upregulated E-cadherin and downregulated vimentin levels. Subsequently, miR-153 upregulation inhibited MKN-45 GC cell migration and invasion, while knockdown promoted the migration and invasion of SGC-7901 GC cells (28).

In conclusion, the serum expression of miR-153 was downregulated in patients with GC, especially in advanced clinical stages. Furthermore, lower expression of miR-153 was associated with larger tumor sizes, poor differentiation, lymph node metastasis and advanced tumor TNM stage, which are associated with poor prognosis. As a result, the findings of the present study suggest that miR-153 may serve as a tumor biomarker and prognostic indicator of patients with GC, as well as a therapeutic target.

**Acknowledgements**

Not applicable.

**Funding**

The present study was funded by the National Science Foundation of China (grant no. 82102398), Shandong Provincial Natural Science Foundation, China (grant nos. ZR2020QC073 and ZR2021MH409), Shandong Provincial Key Research and Development Program, China (grant no. 2019GSF108190), Shandong Province Medical and Health Science and Technology Development Plan, China (grant nos. 2018WS106 and 202103030841), and Weihai Science and Technology Development Plan, Shandong (grant no. 2017GNS11).

**Availability of data and materials**

The datasets generated and/or analyzed during the current study are available in the National Genomic Data Center, China National Center for Bioinformation/Beijing Institute of Genomics, Chinese Academy of Sciences repository (https://ngdc.cncb.ac.cn/gsa-human/; accession no. HRA003675).

**Authors' contributions**

XG and YC were involved in the conception and design of the study. TL, DG, XX and PL retrieved literature and analyzed

data. TL and DG wrote the manuscript, designed the figures and revised the manuscript critically. XX, PW, YZ, LL, YQ and FL were involved in acquisition of data, and analysis and interpretation of data. DG and PL helped with the discussion and corrected the text. TL and DG confirm the authenticity of all the raw data. All authors have read and approved the final manuscript.

## Ethics approval and consent to participate

The present study was approved by the Ethics Committee of Weihai Municipal Hospital (Weihai, China) and written informed consent was obtained from all patients and HCs.

## Patient consent for publication

Not applicable.

## Competing interests

The authors declare that they have no competing interests.

## References


1. Bray F, Ferlay J, Soerjomataram I, Siegel RL, Torre LA and Jemal A: Global cancer statistics 2018: GLOBOCAN estimates of incidence and mortality worldwide for 36 cancers in 185 countries. CA Cancer J Clin 68: 394-424, 2018.
2. Zhao X, Li X and Yuan H: microRNAs in gastric cancer invasion and metastasis. Front Biosci (Landmark Ed) 18: 803-810, 2013.
3. Liu G, Jiang C, Li D, Wang R and Wang W: MiRNA-34a inhibits EGFR-signaling-dependent MMP7 activation in gastric cancer. Tumour Biol 35: 9801-9806, 2014.
4. Matsuoka T and Yashiro M: Biomarkers of gastric cancer: Current topics and future perspective. World J Gastroenterol 24: 2818-2832, 2018.
5. Ambros V: The functions of animal microRNAs. Nature 431: 350-355, 2004.
6. Tang G, Yan J, Gu Y, Qiao M, Fan R, Mao Y and Tang X: Construction of short tandem target mimic (STTM) to block the functions of plant and animal microRNAs. Methods 58: 118-125, 2012.
7. Muhammad S, Kaur K, Huang R, Zhang Q, Kaur P, Yazdani HO, Bilol MU, Zheng J, Zheng L and Wang XS: MicroRNAs in colorectal cancer: Role in metastasis and clinical perspectives. World J Gastroenterol 20:17011-17019, 2014.
8. Chan B, Manley J, Lee J and Singh SR: The emerging roles of microRNAs in cancer metabolism. Cancer Lett 356 (2 Pt A): 301-308, 2015.
9. Romero-Cordoba SL, Salido-Guadarrama I, Rodriguez-Dorantes M and Hidalgo-Miranda A: miRNA biogenesis: Biological impact in the development of cancer. Cancer Biol Ther 15: 1444-1455, 2014.
10. Wang WT and Chen YQ: Circulating miRNAs in cancer: From detection to therapy. J Hematol Oncol 7: 86, 2014.
11. Faam B, Ghaffari MA, Ghadiri A and Azizi F: Epigenetic modifications in human thyroid cancer. Biomed Rep 3: 3-8, 2015.
12. Zhang L, Pickard K, Jenei V, Bullock MD, Bruce A, Mitter R, Kelly G, Paraskeva C, Strefford J, Primrose J, *et al*: miR-153 supports colorectal cancer progression via pleiotropic effects that enhance invasion and chemotherapeutic resistance. Cancer Res 73: 6435-6447, 2013.
13. Hua HW, Jiang F, Huang Q, Liao Z and Ding G: MicroRNA-153 promotes Wnt/β-catenin activation in hepatocellular carcinoma through suppression of WWOX. Oncotarget 6: 3840-3847, 2015.
14. Bi CW, Zhang GY, Bai Y, Zhao B and Yang H: Increased expression of miR-153 predicts poor prognosis for patients with prostate cancer. Medicine (Baltimore) 98: e16705, 2019.
15. Zhao W, Yin CY, Jiang J, Kong W, Xu H and Zhang H: MicroRNA-153 suppresses cell invasion by targeting SNAI1 and predicts patient prognosis in glioma. Oncol Lett 17: 1189-1195, 2019.
16. Guo G, Zhang Y, Hu L and Bian X: MicroRNA-153 affects nasopharyngeal cancer cell viability by targeting TGF-$\beta_2$. Oncol Lett 17: 646-651, 2019.
17. Wang J, Liang S and Duan X: Molecular mechanism of miR-153 inhibiting migration, invasion and epithelial-mesenchymal transition of breast cancer by regulating transforming growth factor beta (TGF-β) signaling pathway. J Cell Biochem 120: 9539-9546, 2019.
18. Zhang B, Fu T and Zhang L: MicroRNA-153 suppresses human laryngeal squamous cell carcinoma migration and invasion by targeting the SNAI1 gene. Oncol Lett 16: 5075-5083, 2018.
19. Wu X, Li L, Li Y and Liu Z: MiR-153 promotes breast cancer cell apoptosis by targeting HECTD3. Am J Cancer Res 6: 1563-1571, 2016.
20. Najtegaal ID, Odze RD, Klimstra D, Paradis V, Rugge M, Schirmacher P, Washington KM, Carneiro F and Cree IA; WHO Classification of Tumours Editorial Board: The 2019 WHO classification of tumours of the digestive system. Histopathology 76: 182-188, 2020.
21. Livak KJ and Schmittgen TD: Analysis of relative gene expression data using real-time quantitative PCR and the 2(-Delta Delta C(T)) method. Methods 25: 402-408, 2001.
22. Sano T, Coit DG, Kim HH, Roviello F, Kassab P, Wittekind C, Yamamoto Y and Ohashi Y: Proposal of a new stage grouping of gastric cancer for TNM classification: International Gastric Cancer Association staging project. Gastric Cancer 20: 217-225, 2017.
23. Zhou J, Xie M, Shi Y, Luo B, Gong G, Li J, Wang J, Zhao W, Zi Y, Wu X and Wen J: MicroRNA-153 functions as a tumor suppressor by targeting SET7 and ZEB2 in ovarian cancer cells. Oncol Rep 34: 111-120, 2015.
24. Luan W, Shi Y, Zhou Z, Xia Y and Wang J: circRNA_0084043 promote malignant melanoma progression via miR-153-3p/Snail axis. Biochem Biophys Res Commun 502: 22-29, 2018.
25. Murai T, Yamada S, Fuchs BC, Fujii T, Nakayama G, Sugimoto H, Koike M, Fujiwara M, Tanabe KK and Kodera Y: Epithelial-to-mesenchymal transition predicts prognosis in clinical gastric cancer. J Surg Oncol 109: 684-689, 2014.
26. Zhang ZY and Ge HY: Micrometastasis in gastric cancer. Cancer Lett 336: 34-45, 2013.
27. Xu Q, Sun Q, Zhang J, Yu J, Chen W and Zhang Z: Downregulation of miR-153 contributes to epithelial-mesenchymal transition and tumor metastasis in human epithelial cancer. Carcinogenesis 34: 539-549, 2013.
28. Zhang Z, Sun J, Bai Z, Li H, He S, Chen R and Che X: MicroRNA-153 acts as a prognostic marker in gastric cancer and its role in cell migration and invasion. Onco Targets Ther 8: 357-364, 2015.